

**UCC Library and UCC researchers have made this item openly available.  
Please [let us know](#) how this has helped you. Thanks!**

|                                    |  |
|------------------------------------|--|
| <b>Title</b>                       | Inverse scattering method design of regrowth-free single-mode semiconductor lasers for monolithic integration  |
| <b>Author(s)</b>                   | Shortiss, Kevin; Dernaika, Mohamad; Caro, Ludovic; Seifikar, Masoud; Peters, Frank H.  |
| <b>Publication date</b>            | 2018-07  |
| <b>Original citation</b>           | Shortiss, K., Dernaika, M., Caro, L., Seifikar, M. and Peters, F. H. (2018) 'Inverse scattering method design of regrowth-free single-mode semiconductor lasers for monolithic integration', Proceedings of Advanced Photonics Congress 2018, Zurich, Switzerland, 2-5 July, ITu4B.4 (2pp). doi:10.1364/IPRSN.2018.ITu4B.4                 |
| <b>Type of publication</b>         | Conference item  |
| <b>Link to publisher's version</b> | <a href="http://www.osapublishing.org/abstract.cfm?URI=IPRSN-2018-ITu4B.4">http://www.osapublishing.org/abstract.cfm?URI=IPRSN-2018-ITu4B.4</a><br><a href="http://dx.doi.org/10.1364/IPRSN.2018.ITu4B.4">http://dx.doi.org/10.1364/IPRSN.2018.ITu4B.4</a><br>Access to the full text of the published version may require a subscription. |
| <b>Rights</b>                      | <b>© 2018, the Authors. Published by the Optical Society of America. One print or electronic copy may be made for personal use only. Systematic reproduction and distribution, duplication of any material in this paper for a fee or for commercial purposes, or modifications of the content of this paper are prohibited.</b>           |
| <b>Item downloaded from</b>        | <a href="http://hdl.handle.net/10468/7670">http://hdl.handle.net/10468/7670</a>  |

Downloaded on 2020-09-23T10:40:58Z

# Inverse Scattering Method Design of Regrowth-free Single-mode Semiconductor Lasers for Monolithic Integration

Kevin Shortiss, Mohamad Dernaika, Ludovic Caro, Masoud Seifikar, Frank H. Peters

Tyndall National Institute, Dyke Parade, Cork, Ireland

Author e-mail address: kevin.shortiss@tyndall.ie

**Abstract:** An inverse scattering method is used to design single moded lasers, using etched depth insensitive pits as perturbations in the laser cavity. We compare 10 pit, 15 pit and 20 pit devices, and report strongly single moded lasers (>40dB). © 2018 The Author(s)

**OCIS codes:** (250.5300) Photonic integrated circuits; (140.3460) Lasers; (140.3570) Lasers, single-mode

## 1. Introduction

The fabrication processes of distributed feedback lasers or distributed Bragg reflector lasers can be expensive and time consuming. In contrast, regrowth-free semiconductor lasers that use standard contact UV lithography greatly reduce the time and cost involved in fabrication, and much research has been focused on improving such devices. Slotted Fabry-Pérot lasers [1,2] can provide high side-mode suppression ratios (SMSR) and low linewidth, however the slots which provide the wavelength selectivity of the laser are etch depth dependent [3]. As a result, etch stop layers are required to accurately control the reflectivity of the slots, and the anisotropy of chemical etches can give different results across a wafer.

In this paper, we demonstrate regrowth-free single moded lasers which use etch depth insensitive pits [4] etched into the waveguide of the slave laser, in order to achieve high spectral efficiency. High SMSR (37dB) and low linewidth have been previously demonstrated using 30 pits in an integrated DBR like mirror [5]. Now, single moded lasing is achieved by using pits as local perturbations of the laser's electric field, as described by an inverse scattering technique [6]. We compare the number of pits required, and report >36dB SMSR achieved in all cases.

## 2. Single moded laser design using an inverse scattering technique

To determine the location of the perturbations required to achieve the target wavelength of 1550nm, and design for a high SMSR, an inverse scattering method was used. As described in [6], the threshold lasing condition for a cavity of refractive index  $n$ , featuring  $N$  perturbations of magnitude  $\Delta n$ , can be written up to first order in  $\Delta n$  as:

$$1 = r_- r_+ e^{2i\sum_j^N \theta_j} + i \frac{\Delta n}{n} \sum_{j=1}^N \sin \theta_{2j} \left[ r_- e^{2i\phi_j^-} + r_+ e^{2i\phi_j^+} \right] \quad (1)$$

where  $r_-$  and  $r_+$  are the field reflection values of the left hand side and right hand side facets,  $\theta_j$  is the change in phase due to section  $j$ , and  $\phi_j^-$ ,  $\phi_j^+$  are the changes in phase when propagating to and from perturbation  $j$  to the left and right facets. We can use the threshold condition above to find the threshold gain of the cavity up to first order:

$$\gamma_m = \frac{1}{L_c} \ln \frac{1}{|r_- r_+|} + \frac{\Delta n}{n} \frac{1}{L_c \sqrt{|r_- r_+|}} \sum_{j=1}^N \sin \theta_{2j} \left[ r_- \sin(2\phi_j^-) e^{\epsilon_j \gamma_m^{(0)} L_c} + r_+ \sin(2\phi_j^+) e^{-\epsilon_j \gamma_m^{(0)} L_c} \right] \quad (2)$$

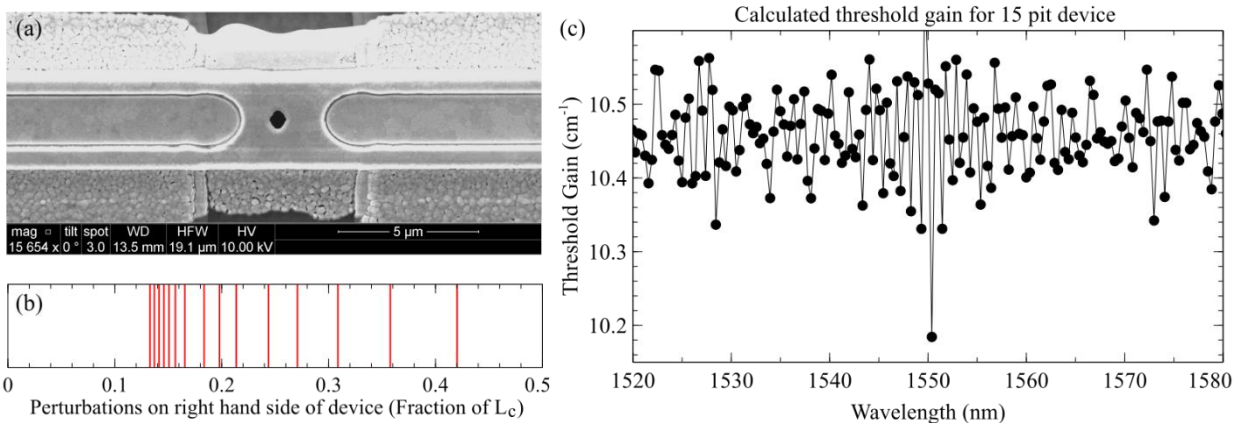


Fig. 1. (a) Electron microscope image of a pit etched into a laser's waveguide. (b) Perturbation locations (as a fraction of the total device length) calculated to target 1550nm, for a 15 pit device. (c) Calculated threshold gain for the grating shown in (b).

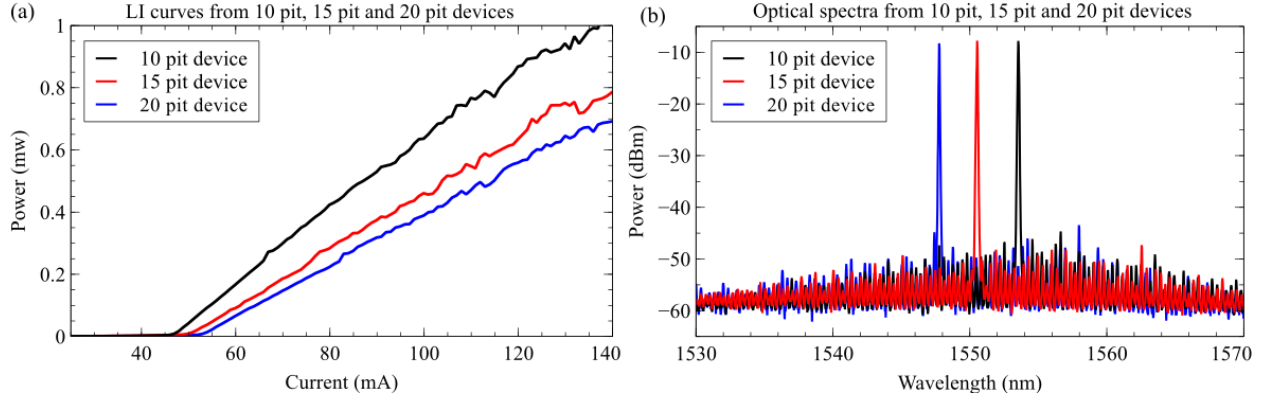


Fig. 2. (a) LI curves for 3 different devices. The bumps in the LI are due to lensed fibre vibrations. (b) Optical spectra from 3 different devices.

where here  $\gamma_m^{(0)}$  is the threshold gain of mode  $m$  in the unperturbed cavity,  $L_c$  is the cavity length, and  $\epsilon_j$  are the fractional positions of the perturbations in the cavity,  $-\frac{1}{2} < \epsilon_j < \frac{1}{2}$ . To determine the positions  $\epsilon_j$  of the perturbations, we first choose a desired threshold modulation function (in this case,  $\text{sinc}(\Delta m)$  was chosen, where  $\Delta m = m_0 - m$  is the difference in wavenumber between cavity mode  $m$  and the target mode  $m_0$ ). The perturbation positions are then calculated by finding solutions to:

$$A \sum_n \int_{\epsilon_{min}}^{\epsilon_j} \left[ r_- \sin(2\phi_j^-) e^{x\gamma_m^{(0)} L_c} + r_+ \sin(2\phi_j^+) e^{-x\gamma_m^{(0)} L_c} \right]^{-1} \Gamma_n(x) dx = j - \frac{1}{2} \quad (3)$$

for  $1 \leq j \leq N$ , and  $A$  is a normalization constant. Here,  $\Gamma_n(x)$  is a series of Gaussians which represent the Fourier transform of the desired threshold modulation function. The term  $\epsilon_{min}$  introduces a lower bound on where the cavity perturbations can be placed. After (3) is used to calculate the initial positions, the perturbations are moved slightly to maximize the  $\sin \theta_{2j}$  term in (1), and then also to take into account the changes in the optical path length due to the perturbations themselves. The pits were assumed to be  $1\mu\text{m}$  wide, with  $\Delta n \approx 0.075$ , and the total device length was  $1\text{mm}$ . The index of refraction of the device was estimated as 3.4. Fig. 1(b) shows the positions  $\epsilon_j$  of the calculated perturbations, and fig. 1(c) shows the corresponding calculated threshold gain for a device with 15 pits.

### 3. Experimental results

The fabricated devices were tested on temperature controlled brass chuck. The light output was collected using a lensed fibre on the cleaved facet side of the device. One side of the device used a metal coated etched facet with estimated reflection of 40%, and the other had a standard cleaved facet. Fig. 2(a) shows the light intensity (LI) curve collected from devices with varying number of pits. The best threshold was recorded in the 10 pit device. Increasing the number of pits featured in the laser cavity increases the total loss in the cavity while also improving the frequency selectivity. Fig. 2(b) shows the optical spectra recorded when each device was biased to 120mA. The 15 pit device achieved a SMSR of  $>40\text{dB}$ , and SMSRs of  $>36\text{dB}$  were recorded in the other two cases.

The lasing wavelength of each laser does not exactly match the targeted 1550nm used in the model above. This is likely due to error in the estimation of the magnitude of the perturbation caused by each pit. Further error is introduced when the devices are cleaved. As the method depends on the optical path length to the facets  $r_-$  and  $r_+$ , errors in the position of the cleaved facet may also effect the lasing wavelength.

### 4. Conclusions

Regrowth free monolithically integrable lasers using deeply etched pits suitable for photonic integrated circuits are presented. A preliminary study on how many perturbations are required to achieve high spectral efficiency was completed, and it was found that SMSRs of greater than 36dB can be achieved (with a SMSR of greater than 40dB recorded in some cases).

- [1] D. C. Byrne et al., "Discretely tunable semiconductor lasers suitable for photonic integration," IEEE J. Sel. Top. Quantum Electron. 15(3), 482–487 (2009).
- [2] B. Corbett, D. McDonald, "Single longitudinal mode ridge waveguide  $1.3\mu\text{m}$  Fabry-Perot laser by modal perturbation" in Electron Lett 31:2181–2182(1995)
- [3] Q. Y. Lu et al., "Analysis of slot characteristics in slotted single-mode semiconductor lasers using the 2-D scattering matrix method", IEEE Photon. Technol. Lett., vol. 16, pp. 2605-2607 (2006).
- [4] M. Dernaika et al., "Deeply Etched Inner-cavity Pit Reflector". IEEE Photonics J. 9 (1), 1–8 (2017)
- [5] M. Dernaika et al., "Regrowth-free single-mode semiconductor laser suitable for monolithic integration based on pits mirror," in Optical Engineering, 56 (8), 086107 (2017)
- [6] S. O'Brien et al., "Spectral manipulation in Fabry-Perot lasers: perturbative inverse scattering approach" J.Opt.Soc.Am. B23,1046-1056(2006).